

Incorporating coarse aggregates into 3D concrete printing from mixture design and process control to structural behaviours and practical applications: a review

Dong An, Y.X. Zhang & Richard (Chunhui) Yang

To cite this article: Dong An, Y.X. Zhang & Richard (Chunhui) Yang (2024) Incorporating coarse aggregates into 3D concrete printing from mixture design and process control to structural behaviours and practical applications: a review, Virtual and Physical Prototyping, 19:1, e2351154, DOI: [10.1080/17452759.2024.2351154](https://doi.org/10.1080/17452759.2024.2351154)

To link to this article: <https://doi.org/10.1080/17452759.2024.2351154>



© 2024 The Author(s). Published by Informa UK Limited, trading as Taylor & Francis Group



Published online: 15 May 2024.



Submit your article to this journal [↗](#)



Article views: 1864



View related articles [↗](#)



View Crossmark data [↗](#)



Citing articles: 4 View citing articles [↗](#)

Incorporating coarse aggregates into 3D concrete printing from mixture design and process control to structural behaviours and practical applications: a review

Dong An , Y.X. Zhang  and Richard (Chunhui) Yang 

Centre for Advanced Manufacturing Technology, School of Engineering, Design and Built Environment, Western Sydney University, Penrith, Australia

ABSTRACT

Three-dimensional concrete printing (3DCP) is progressing from lab pilots to large-scale manufacturing, encountering limitations with conventional printable material – cement mortar. Coarse aggregate concrete (CAC) emerges as a promising alternative due to its superior material properties, cost-effectiveness, and sustainability, attracting considerable interest in academia and industry. This paper explores the integration of CAC into 3DCP, focusing on three critical aspects: mixture design of 3D printable concrete, innovative methods of 3D printing process, and structural behaviours of 3D printed concrete specimens, structural members and systems. It elucidates the relationships among mixture composition, processing parameters, early-age material properties, and printability requirements. Furthermore, particle-bed 3D printing technology for CAC is discussed, highlighting advantages and challenges compared to extrusion methods. Ultimately, this review provides valuable insights into the technical challenges and prospects of 3D printing coarse aggregate concrete (3DPCAC) technology, aiming to foster advancements in research and construction practices.

ARTICLE HISTORY

Received 9 April 2024
Accepted 27 April 2024

KEYWORDS

3DCP; coarse aggregate; mixture design; structural behaviours; practical applications

1. Introduction

Three-dimensional concrete printing (3DCP) is an innovative digital construction method that uses computer-controlled machines to fabricate intricate structures by depositing concrete layers. Gaining attention for its potential to reduce construction time, costs, and material waste, while enabling sustainability and intricate designs, 3DCP is evolving from lab pilots to large-scale manufacturing [1–4]. Research efforts have been made on investigations focusing on optimising material compositions, processing methods, and structural integrity, paving the way for the practical applications of 3D printed concrete structures [5–9].

Traditionally, 3DCP employs cement mortar without the coarse aggregate (CA) to avoid clogging during pumping and extrusion, attributed to the larger particle size (larger than 4.75 mm) and complex properties of CAs [10,11]. However, heightened cement usage raises concerns about increased heat of hydration and shrinkage risks [12,13]. In addition, CAs enhance dimensional stability (higher elastic modulus, mechanical strengths and buildability) and promote economic and ecological sustainability (lower cost and carbon

emission) [14–16]. Incorporating CAs into 3DCP poses challenges but opens new possibilities for superior performances of 3D printed components and structures.

3D printing coarse aggregate concrete (3DPCAC) technology is in its early stages for practical applications. Two main approaches of 3DPCAC are extrusion-based and particle-bed printing technologies [14,17]. The former, extensively researched and applied in the industry so far, is the primary focus here. Particle-bed 3D concrete printing involves the coarse aggregate binding process (CAB) technology, where mortar or paste is selectively deposited onto CA beds to build layer-by-layer structures [17,18]. Additionally, recycled coarse aggregate (RCA) has been explored as an eco-friendly material for 3DCP. Studies [12,19–21] suggested the feasibility of using RCA as a partial replacement of normal coarse aggregate (NCA) in cast and printed concrete, proving its potential to improve the cost-effectiveness and sustainability of 3D printable mixtures.

Recent review papers [2,3,22] highlighted the impacts of CAs on printability and mechanical properties in 3DCP. More reviews on large-scale 3DCP technology

CONTACT Richard (Chunhui) Yang  R.Yang@westernsydney.edu.au  Centre for Advanced Manufacturing Technology, School of Engineering, Design and Built Environment, Western Sydney University, Penrith, NSW 2751, Australia

© 2024 The Author(s). Published by Informa UK Limited, trading as Taylor & Francis Group
This is an Open Access article distributed under the terms of the Creative Commons Attribution License (<http://creativecommons.org/licenses/by/4.0/>), which permits unrestricted use, distribution, and reproduction in any medium, provided the original work is properly cited. The terms on which this article has been published allow the posting of the Accepted Manuscript in a repository by the author(s) or with their consent.

[5,7] indicated that CA competes favourably with fine aggregate (FA) regarding cost, efficiency, and carbon footprint for printing simple geometries. However, these review papers [2,3,5,7,22,23] mainly focused on conventional 3D printing mortar, touching on only one or two aspects of 3DPCAC briefly. One possible reason for this is the recent surge of related research articles [12,19,20,24–34] published within the last 2–3 years, revealing new physical phenomena requiring in-depth analysis. Examples include the impact of CAs on the interlayer bonding of printed concrete layers [19,20,25] and the optimal CA content for desired rheological and mechanical behaviours [27–29]. However, several crucial questions, such as the effects of CA content on yield stress, remain unclear and even conflicting across various publications [12,29,34]. A systematic review of the current literature is essential to consolidate findings and address key aspects of 3DPCAC. However, to the best of the author's knowledge, there was no such a comprehensive review on 3DPCAC technology reported yet.

This study provides a comprehensive review of 3DPCAC technology. The incorporation of CA into extrusion-based 3DCP is explored at three levels: the mixture design of 3D printable material (Section 2), novel methods and control of 3D printing process (Section 3), and structural behaviours of 3D printed specimens, structural members, and systems (Section 4). Additionally, Section 5 introduces the particle-bed 3DPCAC technology and its unique advantages. Finally, Section 6 discusses technical challenges and future directions, while Section 7 presents the summary and conclusions.

2. Mixture design of 3D printable CAC

This section explores the rheological behaviours of fresh coarse aggregate concrete (CAC) and assesses the mixture design to fulfil key printable requirements – pumpability, extrudability, buildability and open time.

2.1. CAC rheology

2.1.1. Rheological behaviours

Rheology is an effective tool to characterise the workability and to predict the flow behaviour of cementitious materials [35]. Fresh CAC, like cement and mortar, behaves as yield stress fluids. The rheological behaviours can be described using the Bingham model [36], which is expressed as.

$$\tau - \tau_y = \mu \dot{\gamma} \quad (1)$$

where τ is the shear stress, τ_y is the static yield stress, μ is the plastic viscosity, and $\dot{\gamma}$ is the shear rate. Fresh

concrete flows only when the applied shear stress τ reaches static yield stress τ_y [37].

Figure 1 illustrates the shearing stress–strain relationships of mortar and CAC, both displaying four stages: elastic, elastoplastic, plastic flow, and flow segments [38]. A significant difference lies in the plastic flow segment. Mortar exhibits a monotonic decrease in the CD segment, indicating residual strength after yielding. However, CAC displays the reappearance of elastic and elastoplastic behaviours in FG and HI segments, suggesting increased residual strength due to the self-locking effect of CAs [39].

CAC exhibits thixotropic behaviours, enabling the yield stress to increase over time [40,41]. Initially, CA has minimal impact on thixotropic structuration, typically within the first 5 minutes after mixing. Beyond this stage, CAC shows a higher thixotropic rate than mortar [20,34,38,42]. The increase in yield stress of CAC over time is commonly considered linear during the first hour of resting [43] and exponential thereafter [44].

2.1.2. Effects of CA on rheological behaviours

Many studies [20,27,31,38,45] suggested that concrete yield stress and plastic viscosity increased with the CA volume fraction due to the self-locking effect of CA and weakened lubrication effect of reduced coated mortar. Recent research [29,42,46] indicated exponential growth in cast and printed concrete with increasing CA content (Figure 2 (a)). This growth can be calculated using the Chateau – Ovarlez – Trung model [42,46] or the Coussot model [29], based on paste yield stress and particle volume fraction. Plastic viscosity can be determined using the Farris model based on the unimodal viscosity of paste, FAs and CAs [47].

However, some studies [12,34] demonstrated that concrete yield stress decreases with the CA content when CA content is low (10% – 30% of total aggregate volume, 6.1% – 18.3% of total mixtures in Figure 2 (b) [34]). This decrease was attributed to a smaller frictional angle and lower uncompacted void ratio [48]. Similarly, in [40,41], appropriately graded aggregate notably reduces yield stress and viscosity. These reductions align with the excess paste theory [49], where concrete contains paste filling spaces between aggregates and excess paste coating and separating aggregates (Figure 3). With low CA content (e.g. 6.1% – 18.3%), hydrodynamic interaction between particles and fluid occurs, resulting in a thicker excess paste layer, smoothing flow, and reducing yield stress. However, in situations with high aggregate volume, concrete rheology is dominated by direct frictional contact between particles. In such cases, CAs impede flow and increase yield stress [50].

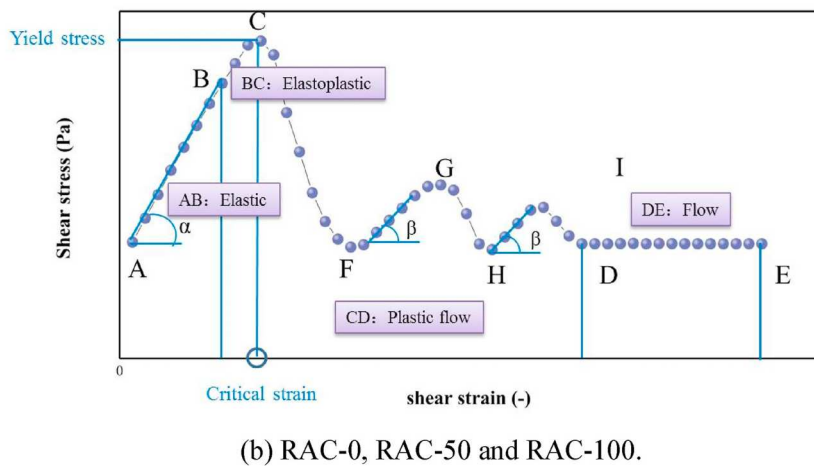
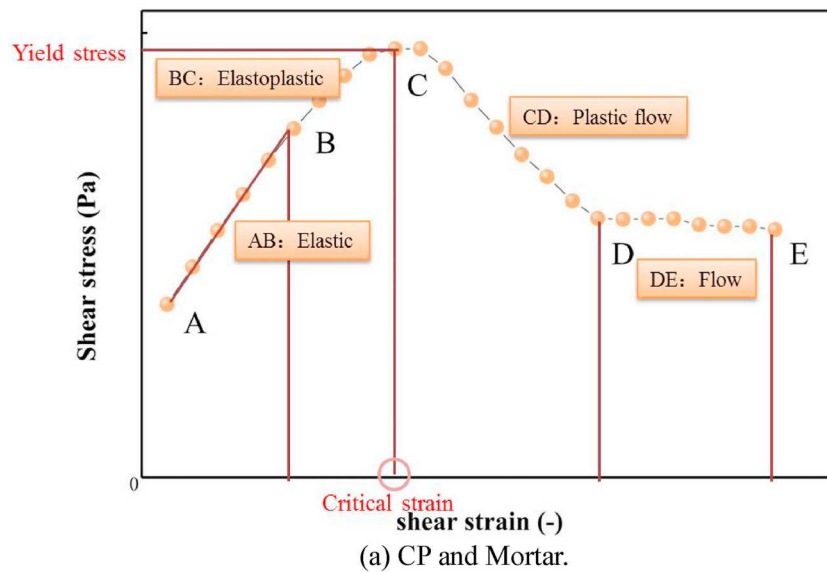


Figure 1. Rheological behaviours of mortar and concrete [38].

It is important to note that the contradicting findings across studies may stem from variations in aggregate gradation and paste compositions. Further research is needed to determine an appropriate aggregate gradation for 3DPCAC, enabling FAs to fill the voids between CAs and achieve an optimal excess paste volume, thus enhancing the rheological and mechanical behaviours of 3D printed CAC.

2.1.3. Recycled aggregate concrete rheology

Recycled aggregate concrete (RAC) exhibits higher static and dynamic yield stress, plastic viscosity and shear modulus than normal aggregate concrete (NAC), attributed to the moisture states, irregular shape and roughness of RCA [28,38,51]. In 3DPCAC, using dry RCAs instead of saturated and surface-dry (SSD) aggregates results in high water absorption [38]. RCAs primarily utilise their water absorption capacity during early ages, significantly reducing the

effective water-cement ratio, workability and opening time [52,53]. For example, RAC, after a 15-minute rest, causes nozzle blockage, unlike the successful printing of NAC [38]. Tong et al. [54] devised a carbonation modification approach coupled with presoaking in nano-SiO₂ solution, resulting in a 21.87% reduction in water absorption, an increase in mechanical strength of 3D printed RAC ranging from 18.27% to 24.71%. Additionally, employing water-reducing admixtures and lower replacement levels of RCA (e.g. 30% by volume [12]) represent two potentially effective strategies.

2.2. Pumpability

Pumpability is a relationship between pressure and flow rate and is related to the initial fluidity of the material [55]. Adequate pumpability ensures the seamless transportation of fresh concrete in pumping systems and

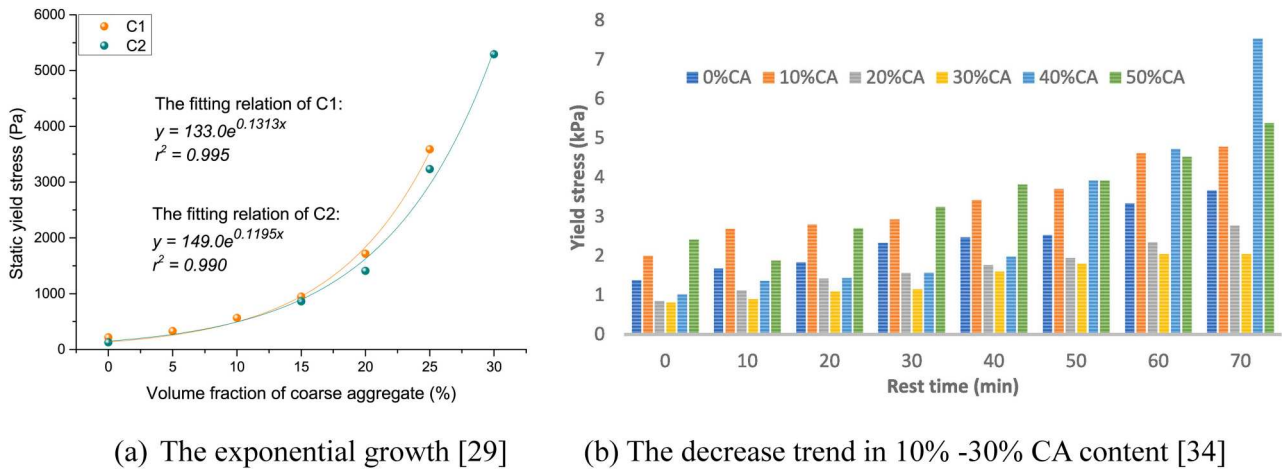


Figure 2. Two typical trends of the yield stress changing with CA volume content.

relies on low or moderate yield stress, low viscosity or forming a lubricating layer.

Figure 4 illustrates the CAC section in the pumping pipe and printhead [20,32]. Concrete flows as slip-flow when the shear stress at the interface between concrete and pipe wall is below the yield stress of concrete. During pumping, the aggregate phase (CAs and FAs) tends to migrate to the plug flow zone (pipe centre), while the paste phase tends to migrate to the shear flow zone (pipe wall) due to the shear-induced particle migration effect, as shown in Figure 4 (a). A lubricating layer (LL) forms on the pipe wall, reducing the shear stress and ensuring a constant flow rate [56]. This minimises pumping pressure, lowers the risk of clogging, and maintains smooth flow. The properties of the lubricating layer, such as its yield stress, plastic viscosity, and thickness, significantly impact the pumpability of concrete.

CAC requires higher starting and flow pressures compared to mortar to ensure smooth transportation [32]. The formation of the CAC lubricating layer takes more

time and depends on the geometry of the pipeline, the trajectory along which the concrete mixture moves, and the shear inside the pipe. Without forming an appropriate lubricating layer at a very early stage, the cement paste might move through the granular matrix, causing the mixture bleeding and pump pipe clogging [57].

2.3. Extrudability

Extrudability refers to smooth and continuous concrete extrusion without blockage or tearing at a given flow rate [58,59]. It also relates to minimal energy consumption during nozzle extrusion [60], quantified by unit extrusion energy (UEE) per volume. In the conventional 3DCP, satisfactory extrudability depends on low yield stress and viscosity. However, for 3DPCAC, special considerations need to be applied.

The crucial factor is the ratio of nozzle size to the CA maximum diameter, with a ratio above 4 preventing clogging [61]. A large nozzle ensures continuous extrusion;

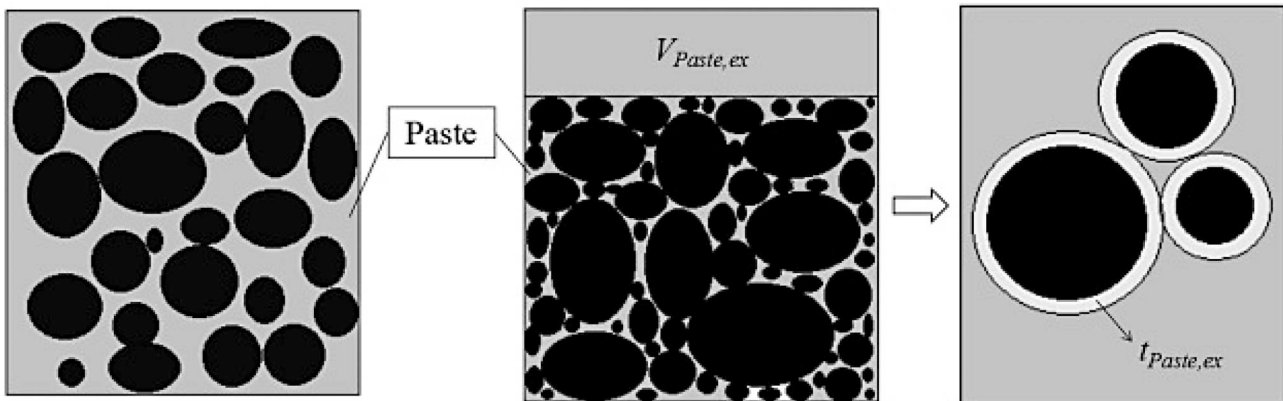
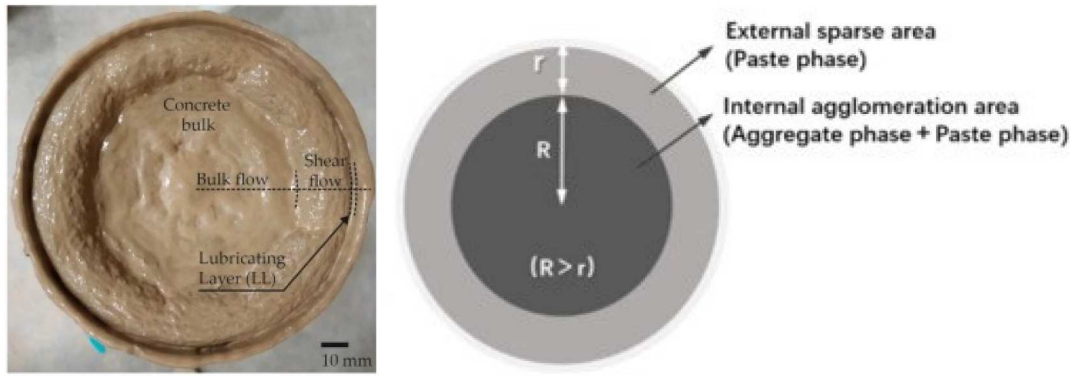


Figure 3. Model of fresh concrete in the excess paste theory [49].



(a) Concrete close-up in the pumping pipe [32] (b) Schematic diagram of concrete in the printhead [20]

Figure 4. The concrete section in the pumping pipe and printhead.

however, ratios below 4 [11,19,38] can cause blocking, leading to paste separation from coarse grains and resulting in poor printing continuity and quality.

Cement and aggregate content also impact extrudability. Researchers generally prioritise cement content in the mix design to wrap aggregates, enabling extrudability and printing quality [62]. Adequate slurry also maintains structural, preventing expansion and vertical slipping of printed concrete structures during stacking and hardening. Chen et al. recommended a cement-aggregate ratio of 0.3 - 0.6 for CAC with a maximum aggregate size of 20 mm, providing good flowability. Wang et al. [27] utilised Ordinary Portland cement (OPC) and sulfoaluminate cement (SAC) to produce 3D printable CAC, finding that a paste-aggregate ratio of 1.3 ensured suitable rheological properties and excellent printing effects.

Once a suitable paste-aggregate ratio is determined, optimising aggregate gradation becomes crucial yet challenging [62]. Extrusion failures were observed with the typical ratio used for cast concrete (cement: FA: CA = 1:2:3) [63] and in lightweight expanded clay aggregates (LECA) concrete with a ratio of 1:0.8:0.7, due to excessive phase separation and diminished water retention capacity. Nevertheless, several methods were proposed to determine the mixture design of 3D printable CAC. Zhang et al. [29] successfully developed a two-phase design strategy based on the composite of mortar and CA, albeit ignoring the gradation optimisation. Taubert and Mechtcherine [64] proposed a generalisable approach to optimise the grading curve by adjusting the mixture components and distribution modulus, facilitating the printing of standard-compliant concrete. However, further design methods and standardisation considerations are needed.

Table 1 summarise the ratio of cement, FA, and CA and other key parameters and properties in 3DPCAC from literature. Figure 5 depicts the ratio of cement,

FA, and CA in concrete from Table 1, serving as an empirical guide for mixture design in 3DPCAC. Blue points represent successful printed mixtures, while blue points with red crosses indicate unsuccessful ones [45,61]. Most blue points fall within a 'Printable zone,' defined by three lines: the X axial, $FA = CA$, and $FA + CA = 3.6$. This indicates that most printable mixtures meet two requirements: (a) CA content is lower or equal to FA content, and (b) total aggregate content is less than 3.6 times the cement content. Requirement (b) implies a cement-aggregate ratio of more than 0.28, consistent with the recommended ratio of 0.3 - 0.6 [11]. Green points show cases [14,24,26,27,51,65] where successful printing occurred with special treatments, including scraper systems and two-stage material handling, discussed in Section 3 allowing for higher CA and FA content in 3D printable concrete.

2.4. Buildability

Buildability is the ability of a material to maintain geometrical stability under sustained and increasing loads [55]. Some studies [11,27,29,38,45] have highlighted that CAs enhance buildability due to their high shear and compressive yield stress, high elastic modulus, high internal friction angle, skeleton effect and dewatering during extrusion. However, as discussed in Section 2.1.2, a few studies [12,34] indicate that CAs reduced yield stress and plastic viscosity and therefore decreased buildability. In such cases, adjusting superplasticiser dosages can help 3DPCAC achieve similar buildability to the control mixture.

2.4.1. Shear properties

Shear properties of fresh concrete are commonly characterised by the Mohr-Coulomb criterion [68], given as.

$$\tau_y = C(t) + \sigma_n \cdot \tan(\varphi(t)) \quad (2)$$

Table 1. Key information of 3DPCAC in literature.

Cement: FA: CA	Extrusion parameters			Rheological behaviours		Printed/cast mechanical strengths after 28 days (MPa)				Study
	$D_{a,max}$ (mm)	D_n (mm)	$\frac{D_n}{D_{a,max}}$	Yield stress (Pa)	Initial flowability (mm)	Compressive strength	Flexural strength	Tensile strength	Surface quality	
1:3.4:0.9	10	150 × 50	5			58.2/57.7 (10 d)	7.45/7.41 (10 d)		Smooth	[14]
1:3.2:3.6 1:3:3.4	15	200 × 100	6.67			24.1/28.8			Smooth	[65]
1:1.3:0.2 1:1.1:0.5	10	30 × 30	3		184 –187				Smooth	[45]
1:0.7:1 1:1:1.5	20	55 × 55	2.75		178–200	64.6/67.6	6.7/7.0		Rough	[11]
1:1.3:2 1:1.4:2										
1:1.8:0.8	9.5	30	3.16		160–210			2.6/2.7	Rough	[10]
1:1:1.5	12	40	3.3	3120 (NAC) 3144 \3884 (RAC)	219–223				Smooth to Rough	[38]
1:2.8:0.8	8							2.2–2.6		[66]
	12	40	3.3	2300–3200		54/66	6.8/7/7		Rough	[25]
1:2:1.3	10	100 × 40	4			42/41	6.2/5.6		Convex	[24]
1:0.6:0.6 1:0.5:0.7	10	40	4			64/54	10.5/6.5	1.8/1.7	Smooth	[27]
1:0.4:0.9 1:0.3:1										
1:2.4:1	8	50 × 20	2.5			33/54	8.7/8.7		Smooth	[12]
1:2.4:2.2	16	150 × 50	3.125						Convex	[26]
1:1:1.5	12	40	3.3	2300–3100 (NAC) 3200–5800 (RAC)		52/65	7/7.8		Rough	[20]
1:1.8:1.26 1:1.8:1.62	10	40	4	3300–3600	150–160	72/78.8			Convex	[29]
1:2:1.2	10	100	10			37/47	5.2/6.0		Convex	[28]
1:2:1.3										
1:1.96:1.3	10	100	10			29/39	6.0/5.1	3.1/2.9	Convex	[51]
1:2.6:0.3 1:2.3:0.6	8	50 × 20	2.5	1360	180				Rough	[34]
1:2:0.9 1:1.7:1.2										
1:1.4:1.4										
1:0.6:1.4	8	100 × 30	3.75			57/55		3.4/3.5	Convex	[31]
1:1.71:1.43 1:1.99:1.41	10	40	4			53.1/37		2.6/2.75	Convex	[67]
1:2.17:0.86										
1:2.46:0.57 1:2.74:0.29										

Note: $D_{a,max}$ is the maximum diameter of CA, and D_n is the characteristic dimension of nozzle, respectively. The listed yield stresses indicate the range when the concrete exhibits a relatively good printing effect. The listed printed mechanical strength is the maximum strength in three directions.

where $C(t)$ is the cohesion force, σ_n is the normal effective, and $\varphi(t)$ is the internal friction angle.

Fresh concrete exhibits higher friction angles and cohesion compared to mortar, primarily attributed to the self-locking effect of CAs. For example, concrete containing 15% CA displays an approximate 8° increase in friction angles, a 1.67 kPa increase in cohesion and a 3.20 kPa increase in yield stress in the first hour [32].

The friction angle and cohesion of fresh concrete typically increase over the rest time. However, a recent study [32] noted an unexpected bi-linear cohesion behaviour of CAC containing 15% CA: the cohesion decreased rapidly in the first hour, followed by a subsequent increase. This unique phenomenon is likely connected to the specific CA volume content (6.1% – 18.3%) discussed in Section 2.1.2.

2.4.2. Compressive properties

The uniaxial compressive stress–strain relationship of CAC evolves from elastoplastic at younger ages to strain-softening at older ages, typical of hardened concrete, as shown in Figure 6 [45]. Barrelling type failure and shear cracks can be found in the specimens of

younger and older ages, respectively. The evolutions of compressive strength and elastic modulus are from linear to exponential growth, as modelled using the Perrot type model [45].

2.4.3. Skeleton effect

Fresh concrete comprises a saturated mix of pore fluid (free water and pore gas), cementitious materials, and an aggregate skeleton. Material deformation and strength only depend on the effective stress from cementitious materials and the aggregate skeleton [10]. CAs act as an internal support framework under external loading: vertically enduring compression and diagonally preventing the formation of shear stress sliding surfaces, significantly increasing material yield stress and buildability.

2.4.4. Dewatering

Dewatering, occurring during extrusion, is a phase separation process similar to the migration effect during pumping but intensified due to accelerated material flow and compaction from reduced printhead diameter [45]. During extrusion, aggregate and paste phases

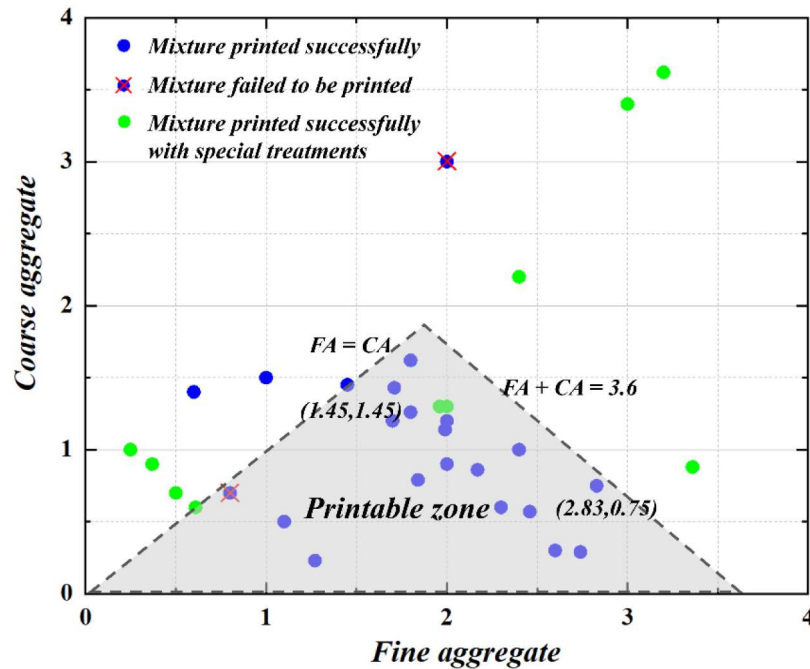


Figure 5. The volume ratios of cement, FA, and CA of 3D printable CAC in [10–12,14,24–29,31,34,38,45,51,61,65–67].

become layered within the filament, with the external sparse area dominated by the paste phase with a high water-cement ratio (see Figure 4 (b)) [20]. This area, characterised by lower cohesive force, affects both fresh and hardened mechanical properties. The water-retaining capacity of the mix can be evaluated by the desorptivity. Compared with mortar, the CAC shows a 23 - 39% decrease in desorptivity when the CA content is 15 - 45% [45]. While phase separation is inevitable,

proper management enhances buildability and surface quality, as the external paste phase provides a smoother surface compared to CA. However, excessive dewatering, often due to high CA content, challenges extrudability and surface quality.

2.5. Printability

Figure 7 depicts the relationship among composition design (material parameters), processing parameters, early-age material properties and printability in 3DPCAC. The **bolded** aspects demand special attention in 3DPCAC considerations. Material and processing parameters distinctly shape the material properties of fresh CAC, with a focus on satisfying printability requirements. However, inherent material traits of CAC, such as high yield stress, viscosity, internal friction angle, and the skeleton effect, enhance buildability while challenging pumpability and extrudability [45]. To address this issue, a specially designed admixture composition, alongside optimised processing parameters and novel technology (discussed in Section 3), is essential.

For a tailored composition design in printable CAC, a key strategy involves utilising diverse mineral and chemical additives to reconcile the inherent conflicts among pumpability, extrudability, and buildability. Table 2 outlines additives used in 3DPCAC and their impacts on rheological and other behaviours. Additives like metakaolin, recycled power, hydroxypropyl methylcellulose (HPMC) and early strength agent (ESA)

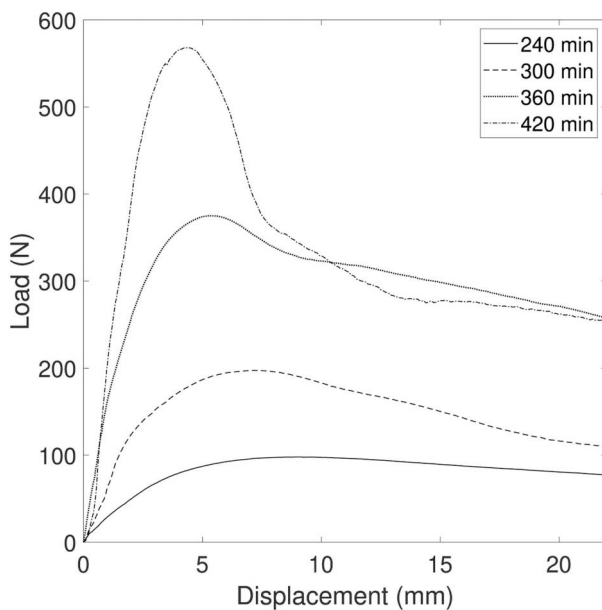


Figure 6. Concrete evolution from elastoplastic type to strain softening type [45].

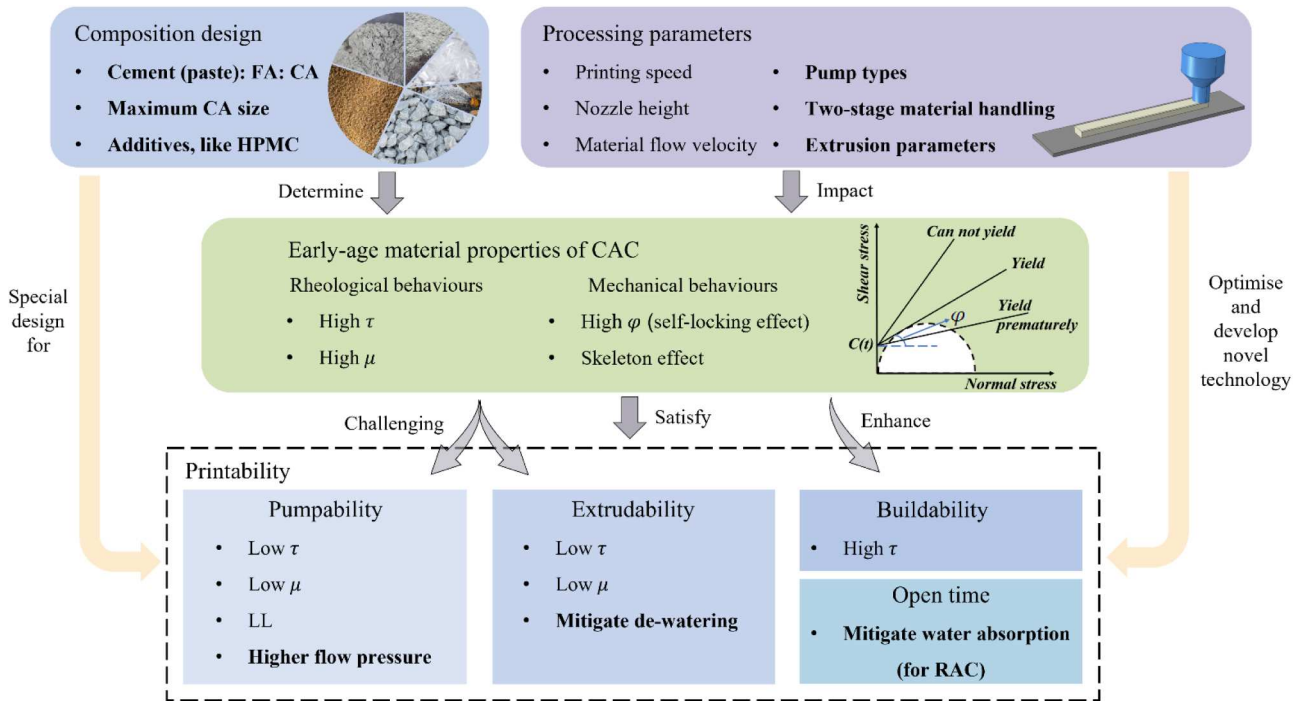


Figure 7. The relationship among material and processing parameters, early-age material properties and printability in 3DPCAC.

enhance concrete strength but diminish workability [38,51,66,69–71]. Notably, HPMC plays a crucial role in the composition design of printable CAC. It acts as a viscosity-modifying agent by swelling and thickening effect, transforming the concrete from low yield stress and low plastic viscosity to high yield stress and moderate plastic viscosity [51]. It also improves the water retention capacity post extrusion, avoiding the bleeding and

Table 2. Effects of various additives on rheological and other behaviours of concrete.

Additives	Effect on rheological behaviours	Other main effects on concrete
Metakaolin	Increasing yield stress and viscosity, and reducing workability	Increasing compressive and flexural strengths
Recycled power		Increasing mechanical properties
HPMC		–
ESA	Increasing structuration rate	Increasing early strength
SF	Increasing pumpability	Increasing compressive strength, bond strength, and abrasion resistance
GGBS	Uncertain effect on yield stress and decreasing plastic viscosity	Increasing durability
FA	Reducing yield stress significantly and viscosity moderately, and improving workability	–
SP	Reducing workability, but can be compensated with SP	Overcoming interlaminar degradation
PVA fibre		
PE fibre		
PP fibre		
Basalt fibre		
Steel fibre		

blockages caused by CAs. Regarding silica fume (SF), its impact on yield stress and plastic viscosity varies [67]. While many studies [72–74] suggest an increase, others [75,76] propose a reduction, contingent on specific superplasticizer (SP) and water-cement ratios. Generally, SF can enhance concrete pumpability by filling voids between particles and increasing lubrication effects [35].

On the other hand, fly ash (FA) and SP can significantly decrease yield stress and moderately reduce plastic viscosity, thereby improving flowability. Ground granulated blast-furnace slag (GGBS) generally decreases plastic viscosity, but its effect on yield stress is uncertain [12,34,35]. Effectively reducing viscosity with additives remains challenging and requires further study [29].

Various fibres, including polyvinyl alcohol (PVA), polyethylene (PE), polypropylene (PP), steel, and basalt fibres, were used to overcome interlaminar degradation and improve buildability and mechanical strengths of 3D printed CAC [10,12,31,34,38,77]. Although these fibres reduce workability, this effect can be mitigated by SP [78,79]. In addition, CAs lead to divergence and the weakened orientational alignment of fibres [77].

To evaluate the printability of CAC before actual printing and optimise the additive formulations, various rheological indicators used for assessing the workability of cast concrete can be employed, including yield stress, (initial) flowability, and slump. As shown in

Table 1, the static yield stress of printable NAC generally falls within the range of 2300 - 3600 Pa, which is higher than that of mortar (2100 - 2700 Pa) and lower than the corresponding RAC (3200 - 5800 Pa) [20,25,29,38]. The typical dynamic yield stress of CAC is around 900 Pa [29,34]. Note that the yield stress increases over time, and the listed values represent the stress when the concrete exhibits a relatively good printing effect. For mortar and NAC, the time is typically around 10 mins after mixing, while for RAC, it is about 5 mins due to higher water absorption [38].

Zhang et al. [29] suggested that residual slump and flowability correlate well with static and dynamic yield stresses of CAC, respectively. Studies [38,45] showed that the initial flowabilities of mortar and CAC are similar, but they differ by about 4 - 20% after 15 mins, depending on the CA type and content. Many studies [10,11,34,38,45] recommended an initial spread range of approximately 160–210 mm that meets the flowability and buildability requirements of 3DPCAC.

3. 3D printing process control for CAC

In the conventional 3DCP, processing parameters like printing speed, nozzle-to-layer height, and material flow velocity have a notable impact on printed material properties and geometry. However, in 3DPCAC, the focus shifts to ensuring extruding continuity and satisfactory surface quality. Factors like pump types, two-stage material handling, and extrusion parameters should be carefully considered.

3.1. Pump types

Due to the higher starting and flow pressure required in 3DPCAC, using conventional positive displacement pumps for 3DCP to pump CAC is challenging [80]. To overcome this barrier, Rahul et al. [45] adopted a long, slow-moving piston-pump-based system, allowing larger aggregates to migrate inwards and embed within the binder during extrusion. Additionally, CON-Print3D technology utilises rotor pumps that provide a smoother, more uniform, and nearly shock-free material flow to the printhead, reducing pumping mast oscillations compared to common piston pumps [14].

3.2. Two-stage material handling

Two-stage material handling involves adding additives to concrete during mixing and on the printhead [14,81]. These additives, such as HPMC, typically increase yield stress and viscosity. Incorporating them on the printhead can enhance buildability and mitigate their

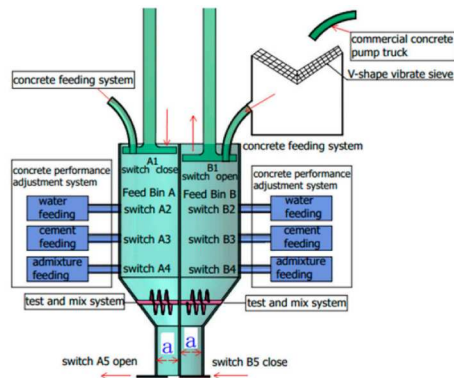
impacts on pumpability and extrudability. Ji et al. [65] developed a double-assisted print head, achieving two-stage material handling and uninterrupted concrete printing (Figure 8 (a)). Xiao et al. [51] printed RAC with a 90–110 mm slump through secondary mixing of HPMC. This secondary mixing results in a greater increase in static yield stress compared to 30 minutes of resting and higher HPMC dosages. Furthermore, Wang et al. [27] used a secondary high-precision pressure pump to introduce admixtures into flowing concrete in the extruder, successfully printing CAC.

However, these methods raise printhead weight, challenging pump mast stability and printing precision, especially with high CA content and printing rates [14,27]. Refining drive components, control algorithms, and control systems [82] are vital to address these concerns and enhance the robustness of printing systems.

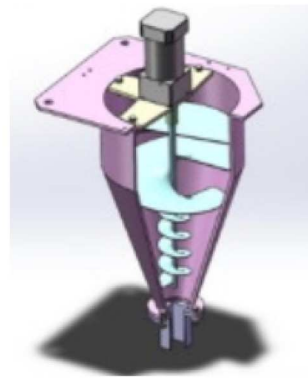
3.3. Extrusion parameters

Extrusion parameters, including the dimension, shape and direction of the nozzle, extrusion method and scraper, significantly affect the extrudability, mechanical properties, and surface quality of 3D printed concrete. For effective extrusion, the nozzle dimension should be at least four times larger than the CA diameter, making rectangular nozzles preferable for 3DPCAC due to their capacity to accommodate larger lengths, typically ranging from 50 mm to 200 mm [12,14,24,26,65]. Rectangular nozzles also produce concrete with smoother surfaces and lower porosity [83,84]. Regarding nozzle orientation, vertical nozzles are commonly used since extrusion pressure helps redistribute the CA and reduces pore diameter, enhancing compactness and strength, especially flexural strength [27,65]. Conversely, horizontal nozzles weaken the interface bond [85].

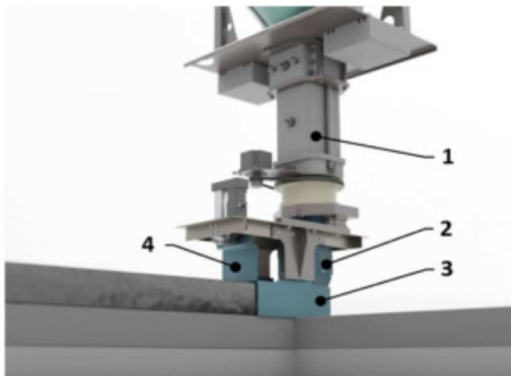
Ram and screw extrusion are two common extrusion methods in 3DCP [23]. However, extruding CAC poses challenges for both, necessitating modifications. Traditional ram extrusion may generate a dead zone in the printhead [86], disrupting the continuous extrusion of CAC. To address this, Ji et al. [65] developed the double-assisted print head (Figure 8 (a)). On the other hand, screw extrusion can interfere with hydration product nucleation in concrete, reducing the yield stress and improving flowability [24]. However, larger particles may jam in the hopper and screw. To solve this problem, Chen et al. [11] used delivery blades to transport concrete and utilised spirals to generate concrete shear thinning (Figure 8 (b)). Additionally, vibrating the nozzle and storage bin before printing can also rapidly reduce concrete yield stress, facilitating extrusion [87,88]. Wang et al. [27] attached a vibration motor to



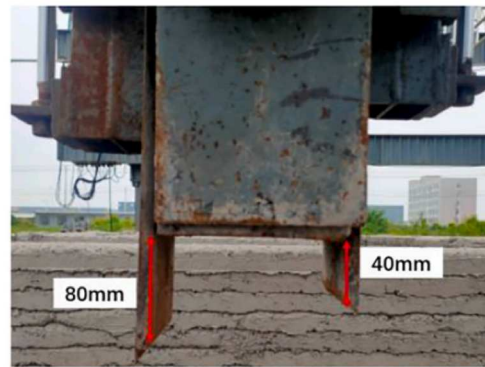
(a) The double-assisted print head [65]



(b) Screw-extrusion developed in [11]



(c) Horizontal nozzle with scraper system [14]



(d) Automatic height-adjusting scraper system [24]

Figure 8. Various extrusion systems developed for 3DPCAC.

the storage bin, ensuring continuous vibration during concrete extrusion and resulting in improved mechanical properties compared to cast concrete.

The scraper system, originally from the Contour Crafting [89], is increasingly used in 3DPCAC to enhance surface quality [14,27]. In the CONPrint3D technology (Figure 8 (c)), shaping plates maintain smooth printed filaments, while a shutter and multiple actuators allow diverse wall cross-section printing [14]. Scrapers prevent excessive concrete spreading, improving mechanical properties and filament geometry. Furthermore, Ji, et al. [24] developed an automatic height-adjusting scraper system (Figure 8 (d)) to accommodate longer scrapers, which could further optimise performance [24].

4. Structural behaviours of 3D printed CAC and practical application

4.1. Anisotropic mechanical strengths

The practical application of 3D printed CAC structures predominantly relies on the hardened properties of

printed concrete, including mechanical strengths, structural behaviours, surface quality and shrinkage.

CA improves compressive, flexural, and splitting tensile strength and elastic modulus of concrete in young and old age, attributed to CA increasing internal friction angle and aiding dewatering during extrusion [27,45,65]. The increase in flexural strength is particularly significant due to enhanced crack resistance and fracture behaviours [27,66,90]. An optimal CA dosage exists for the development of compressive and flexural strength in printed or cast concrete; surpassing this threshold results in diminishing strengths [91]. Studies of 3DPCAC [27,29,45] demonstrated that CA content of 25%, 25%, and 20%, respectively, resulted in 11%, 25%, and 45% to 60% increases in compressive strength compared to mortar. Machine-learning technology, specifically Support Vector Machine, was employed to predict the flexural and tensile strengths of 3D printed CAC based on data from 25 literature studies, though the small sample size posed a risk of overfitting during training [92].

3D printed CAC specimens are generally weaker than cast concrete due to introduced pores, weak interlayer bonds, and lower density, as shown in Table 1.

However, some studies [27,31] achieved 3D printed CAC with lower porosity and improved mechanical properties compared to cast concrete, attributed to suitable material properties and printing processes.

Anisotropy is inherent in layer-by-layer 3D printing, with patterns influenced by aggregate combination, processing parameters and the resting time [93]. Typical compressive strength patterns for 3D printed CAC are $X > Y > Z$ axis [20,25,27] and $Z > X > Y$ [12,51], while for flexural strengths, common patterns include $Y > Z > X$ [11,12,24,28,51] or $Z > Y > X$ [20,25]. The anisotropy can be quantified using an anisotropy coefficient [94]. Compared to mortar, the coefficient for 3D printed CAC is lower, attributed to CAs penetrating interfaces and bridging neighbouring layers, enhancing material strength [27].

Liu et al. [19,20,25] extensively investigated the anisotropy, pores, and interlayer bond of 3D printed hardened NAC and RAC and they proposed the multiple partition-interface model and filament interfacial bonding system. It was found that, compared to mortar, 3D printed CAC exhibits larger pores with more pronounced boundary angles (irregular geometry) and lower compactness. These pores are generally flat and ellipsoidal, differing from the spherical pores found in cast concrete, attributed to uneven, porous CAC filament surfaces, hindering fusions between filament interfaces. The unique pore geometry induces crack initiation and propagation, causing weakly bonded interfaces and leading to anisotropy.

Despite for causing large, irregular pores, CAs significantly enhance the interlayer bond strength, surpassing that of mortar. For instance, the splitting tensile strength of 3D printed CAC in [25] was more than double that of mortar. Splitting tensile tests in [27,95] revealed aggregates splitting at the interface of the broken specimen, indicating that CAs penetrate the interface, bridge layers, and widen the force transfer path, ultimately improving the bonding strength.

3D printed RAC possesses slightly inferior mechanical properties compared to 3D printed NAC, mainly due to the lower mechanical properties of old mortar aggregates. However, two factors partially offset this decrease: (a) the rougher surface of RCA, which enhances bonding with mortar, and (b) the high water absorption and substantial cement content of the old mortar, reducing the local water-cement ratio around the RCA [20].

4.2. 3D printed early-age specimens and structural behaviours

Strength, stiffness, and stability are crucial aspects of structural design. 3D printed early-age CAC multilayer structures typically fail in two modes – (strength-

based) plastic collapse and (stability-based) elastic buckling.

Plastic collapse occurs when concrete stress reaches its yield point, via compressive or pressure-dependent shear failure, defined by the maximum stress and Mohr-Coulomb theories, respectively [96]. Compression failure stems from constituent crushing (Figure 9 (a)) [38], while shear failure results from particle shear movement (Figures 9 (b) and (c)) [10]. The inclined plane failure is common in 3D printed mortar specimens, where shear strength is mainly provided by the cohesion of the cementitious material. The multi-crack failure occurs in 3D printed CAC specimens, with shear resistance stemming from both the cohesion of the cementitious materials and the friction and bite force of the aggregates.

Figure 10 compares the early-age compressive load – displacement curves of 3D printed mortar and CAC multilayer structures (see Figures 9 (b) and (c) for their respective failure modes) [10]. The CAC structure has a bearing capacity five times larger than that of mortar counterpart, highlighting the pronounced effects of the aggregate skeleton on enhancing yield strength and buildability. Moreover, the CAC curve exhibits an S-shaped profile, with three distinct stages: (a) Initial stage showcases high bearing capacity and minimal deformation, crucial for constructability; (b) Upon surpassing the ultimate bearing capacity, mid-term bearing capacity is achieved, marked by marginal load-bearing capacity variation and large deformation, leading to gradual structural degradation within a material failure zone, and (c) Later loading stages witness a more compact internal particle size, resulting in a rapid increase in the load-bearing capacity.

Elastic buckling occurs due to a loss of equilibrium of forces and moments, initiating uncontrolled deformations or displacements, and is controlled by the material shear modulus G and structural geometry. Table 3 provides analytical solutions for three failure modes of 3D printed concrete structures. Equations (3) and (5) predict the maximum printed height of plastic collapse and elastic buckling, respectively [55,97], although Equation (5) may underestimate elastic buckling [38,45]. Equations (4) and (6) are their rewritten forms considering 3D printing process parameters and structural geometry, respectively: the left side of the two formulations relates to material parameters, while the right side relates to process parameters [38]. These formulations enable rough estimations of the maximum printed height and buildability of 3D printed CAC structures based on material yield stress and shear modulus. For example, compared to mortar mix, 3D printed CAC exhibits a 45–60% increase in

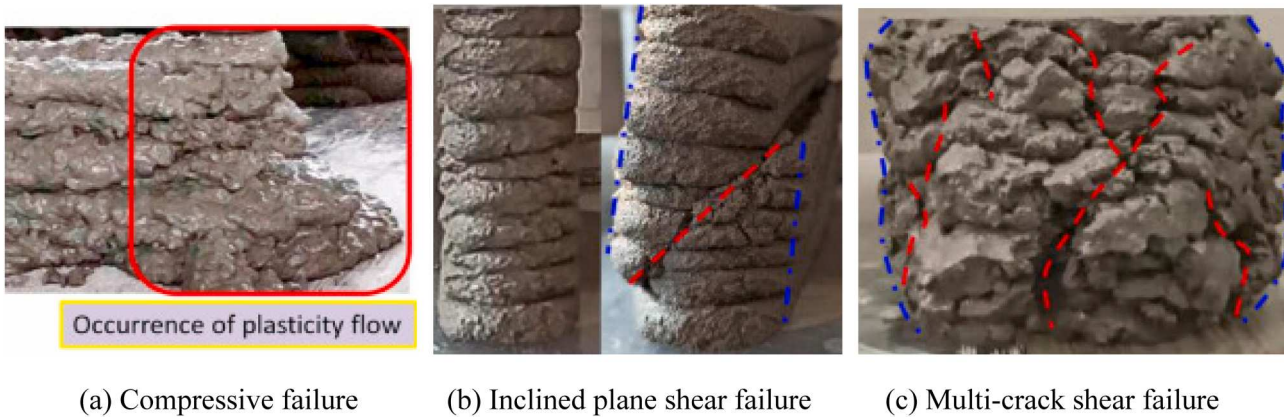


Figure 9. Plastic collapse of 3D printed concrete specimens [10,38].

compressive yield stress and a 25–50% increase in elastic modulus, resulting in 56–72% and 10–17% increases in critical height considering plastic collapse and elastic buckling, respectively [45].

Figure 11 compares Equations (3) and (5) in the same coordinate system, illustrating the required yield stress and shear modulus for the successful printing of a specific object [38]. Yield stress governs successful printing when the printing height is below the critical threshold, while shear modulus becomes crucial beyond this height. As the demand for shear modulus increases cubically with height, it is more sensitive to changes in height. Compared to mortar, CAC necessitates a higher shear modulus due to its increased density. Precise control of printing settings is vital to prevent premature elastic buckling. In cases where increasing shear modulus cannot meet requirements, engineering applications may resort to batch printing and assembly moulding.

Concerning stiffness-based failure, Equation (7) [55] defines the critical shear modulus G to prevent excessive

deformation. 3D printed concrete multi-layer structures lose height due to gravitational loads, with the bottom layer experiencing the most deformation. This deformation extent can be evaluated by the shape-stability test. Higher CA and reduced slurry contents result in the deformation increased due to lower material density and inadequate slurry to envelop and restrict the flow of CA [11]. However, stiffness-based failure is less prominent in 3DPC, and there is a lack of defined failure criteria. One reason might be that when accumulated layer deformation becomes excessive, extra layers can be printed to reach the desired height.

4.3. 3D printed hardened structural members and large-scale structural systems

Some mortar structures include buildings, bridges, and other civil infrastructure have been successfully 3D printed [98,99]. However, to withstand structural loads such as static, wind, snow, and seismic forces, 3D

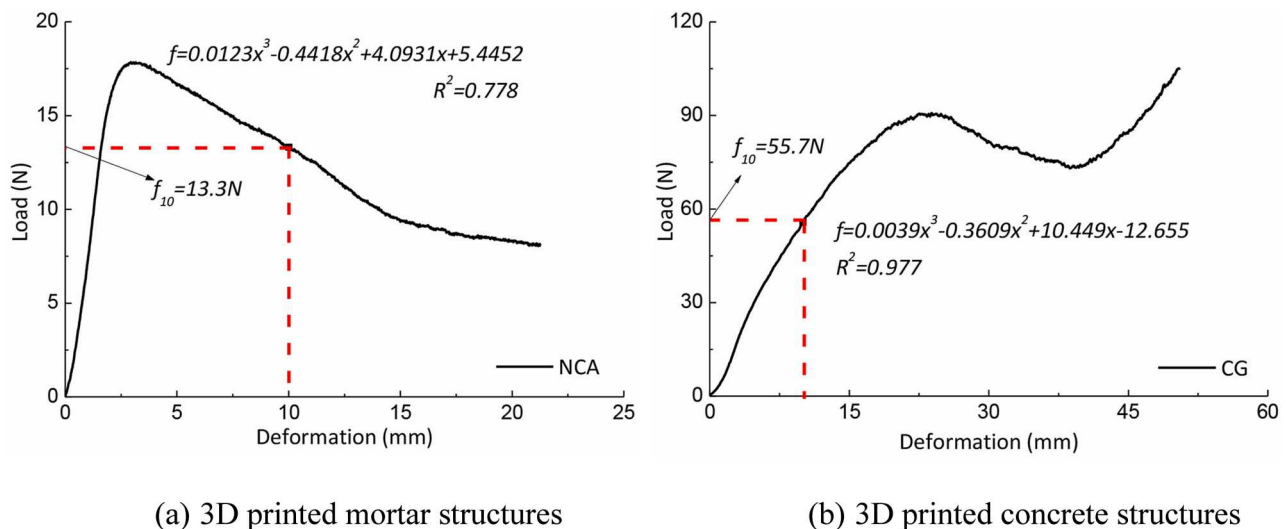


Figure 10. Compressive load – displacement curves of 3D printed multilayer structures [10].

Table 3. Analytical solutions of three failure modes of 3D printed concrete structures.

Failure mode	Analytical solution
Plastic collapse	$H_c = \frac{\tau_c(t)}{\rho g}$ (3)
	$\tau/\rho g = Vh_0 t / \sqrt{3S}$ (4)
Elastic buckling	$H_c = \left(\frac{8E(t)I}{\rho g A} \right)^{\frac{1}{3}}$ (5)
	$G(1 + \nu)/\rho g = 3H^3/4\delta^2$ (6)
Stability-based failure	$G = \rho g h_0 / \gamma_{tol}$ (7)

printed concrete structures must integrate CAC and reinforcement to prevent catastrophic brittle failure. Despite advancements, the application of 3D printed CAC structures is still in emerging stage. Two common construction methods widely adopted so far are print-in-place (PIP) and preprint [79,100]. PIP, the focus here, generally offers higher efficiency and lower costs compared to the preprint, which resembles prefabricated buildings with limited transportability. One typical PIP production process involves printing hollow walls or columns as formworks and subsequently filling them with concrete. Chen et al. [101] printed permanent CAC formworks of structural components with a splitting tensile strength of 2.3–4.4 MPa, surpassing 3D printed mortar formwork by 1.2–3.3 MPa. However, these formworks displayed shear fractures in the interlayer under compression loads, leading to main crack development and extensive spalling from the core concrete. To address this, they devised a novel square stirrup with reserved reinforcement holes built into the 3D printed permanent formwork, enhancing printed column performance, as shown in Figure 12 (a) [30].

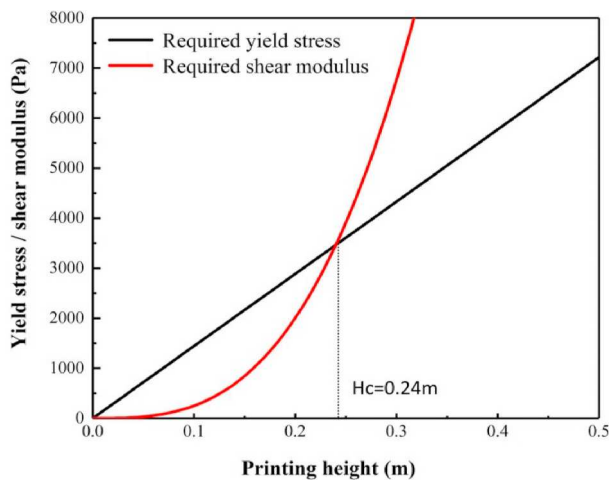
**Figure 11.** Required yield stress and shear modulus as a function of printing height [38].

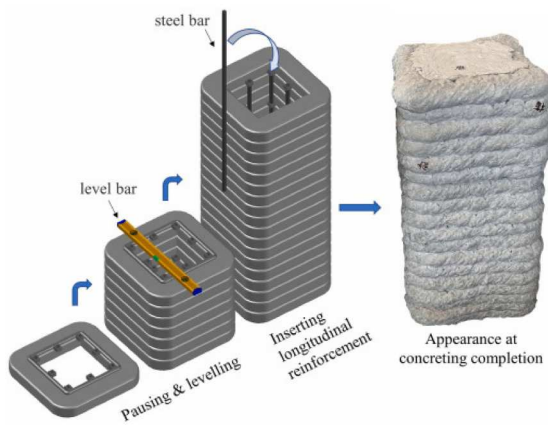
Table 4 summarises key large-scale practical applications of 3D printed CAC structures. The US Army Corps of Engineers [102,103] constructed semi-permanent B-Hut structures, showcasing continuous CAC printing with optimised geometries and reinforcement. Engineered to endure ASCE 7 design loads, traditional concrete foundations and roofs were used with 3D printed walls. Wall contours were printed onto foundations and anchored using steel angles and bolts. Upon reaching 28-day strength, walls were filled with self-consolidating concrete (SCC), and L-hook anchors were installed for roof connection. Chevron wall geometry (Figure 12 (b)) was used for optimising space utilisation and reinforcing placement. Additionally, NASA [104] developed Additive Construction with Mobile Emplacement (ACME) technology for lunar and Martian infrastructure, executing prototypes and full-scale additive structural construction with CAC and indigenous materials.

Ji et al. [65] printed a power distribution substation using C25 ready-mixed CAC, incorporating constructional columns and ring beams to meet seismic requirements. They first printed underground structures, including the cable trench, equipment foundation, and oil collection tank, along with the wall. Constructional columns were then constructed using supporting formworks, steel bars, and casting concrete. Furthermore, a Chinese construction company, HuaShang Tenda, 3D printed a two-storey house on-site, built to withstand earthquakes up to magnitude 8 on the Richter scale [105]. The house frame, with rebar support and plumbing pipes, was erected first. Then, 250-mm-thick walls were printed using ordinary C30 concrete. The printer used a forked extruder to simultaneously lay concrete on both sides of the steel reinforcement, encasing it within the walls.

In those above-mentioned cases, horizontal and vertical steel bars or mesh were strategically placed in the (reserved) concrete hollow or between layers before, during or after printing to bolster structural integrity. It has been found that bond strengths between 3D printed CAC and steel bars exceed those of mortar and parallel placement of rebar and printed segments shows stronger bond strength than vertical ones [106]. However, all reinforcement applications were manual, underscoring the pressing need for further automation development.

4.4. Economic and environmental benefits

3DPCAC technology offers a cost-effective, eco-friendly alternative to traditional concrete construction. It significantly reduces construction time and manual labour



(a) 3D printed CAC formwork [30]



(b) B-Hut structures with Chevron wall geometry [102]

Figure 12. 3D printed CAC structural members and structures.

while also minimising waste and dust pollution. Traditional methods often allocate 35–60% of expenses to formwork material and labour costs [9], which can be saved with 3DPCAC. Printing the main building component usually consumes only one-tenth of the total construction time, resulting in a 60–80% reduction compared to casting concrete [65,103]. However, practical construction issues such as pump wear and material blockages can cause printing stoppages and exacerbated evaporation drying effects. Continuous printing with robust equipment and efficient project scheduling further reduce delay time and overall construction duration [102,103].

Regarding the environmental impact, 3DPCAC can substantially reduce the carbon footprint while 3DCP generally has higher carbon emissions than traditional concrete construction, due to higher cement content [14,108]. The Portland cement and cement mortar release around 0.82 and 0.24 kg CO₂ equivalent (kg CO₂/kg product), respectively, while typical CAC and

reinforced concrete are about 0.14 and 0.18 kg CO₂ equivalent, respectively [5]. Furthermore, incorporating RCA into 3DPC shows both environmental and economic benefits since (a) RCA can reuse construction waste and (b) the price of RAC is much lower than NAC and the main cost of 3DPC is building materials [108].

4.5. Surface quality and shrinkage

The surface quality of 3D printed CAC structures in Table 1 is categorised into three levels: smooth, convex, and rough, based on close-up observations in the literature, as shown in Figure 13. Rough surfaces are common in 3DPCAC, with typical defects such as voids, cracks, exposed aggregate, intralayer fracture, and continuous interlayer fracture [11,45,109], potentially leading to significant durability and impermeability losses [11]. Excessive CA content is a primary cause of poor surface quality, leading to inconsistent movement of CAs and

Table 4. Key information of large-scale 3D printed CAC structures

Application	Concrete	Reinforcement	Construction flow	Design level	Building size and time
B-Hut structures [102, 103]	5000 psi (34.5 MPa) concrete with the maximum aggregate size of 9.5 mm	Horizontal bars at the bottom and top of walls; vertical steel bars in the wall core	1. Casting concrete foundations with reinforcement. 2. Printing wall contours with placing reinforcement. 3. Filling the wall hollow using SCC. 4. Connecting precast roof	ASCE 7	a 512 ft ² (16 ft x 32 ft x 9.25 ft) in 5 days
The power distribution substation [65]	C25 ready-mixed concrete with 5–15 mm CA	Horizontal steel mesh in walls at a 500-mm interval; steel cage in constructional columns	1. Printing the underground structure and wall. 2. Constructing the constructional columns	–	55.66 m ² (12.1 m x 4.6 m x 4.6 m) in 35 days (54 days for cast concrete)
The two-storey house [105]	Ordinary C30 concrete with 5–20 mm CA	Horizontal and vertical steel bars	1. Erecting house frame with rebar support and plumbing pipes. 2. Printing walls	Level 8 earthquake resistant	400 m ² in 45 days
The six-storey apartment [107]	RAC	Horizontal and vertical steel bars	1. Placing pre-printed wall. 2. placing beam columns and steel rebar within the walls	–	1100 m ²

mortar during pumping and extrusion, resulting in inadequate mortar filling gaps and the formation of pits and tears in the printed strips [27]. Table 1 also presents instances of smooth 3D printed CAC specimens, achieved through various methods such as reducing CA content [45], increasing nozzle size [14,24,65], and applying special treatments on the nozzle, like scrapers [14,24].

Shrinkage significantly affects concrete volume deformation, cracking, and durability. Shrinkage development in printed CAC (e.g. 500 - 1000 $\mu\text{m}/\text{m}$ in 8 hours [10]) is much faster than cast CAC (e.g. 600 - 750 $\mu\text{m}/\text{m}$ in 8 days [12]), due to the higher cement content in printable material and the lack of formwork [110]. It is found that increasing CA content reduces chemical and autogenous shrinkage by decreasing cement paste and restrains dry shrinkage [111]. However, limited studies on the shrinkage behaviour of 3D printed CAC exist, partly due to practical difficulties in experiments such as attaching 'DEMEC pins' to printed samples [12]. Bai et al. [10] carried out non-contact and contact shrinkage tests to evaluate shrinkage behaviours of 3D printed RCA, revealing adverse effects of the printing process and aggregate types. A more profound analysis is imperative for a comprehensive understanding of 3D printed CAC shrinkage behaviours.

5. Coarse aggregate binding process

The coarse aggregate binding process (CAB) is a new advancement in particle-bed 3DCP. In this method, cementitious material filaments are selectively deposited onto CAs bed to form layer-by-layer structures [112]. The deposition of mortar or paste can be achieved either by extruding, as demonstrated in Aggregate-bed 3D concrete printing (Figure 14 (a)) [17] or by spraying, as in Large Particle 3D Concrete Printing (Figure 14 (b)) [6].

The particle-bed 3DCP process involves two repetitive steps: applying dry particles and selectively binding the particle layer by locally depositing fluid. Non-bonded particles are removed in the de-powdering process [113]. Shi et al. [17] extended this concept to aggregate-bed 3DCP, printing CAC with 40% CA content and achieving compressive and flexural strengths up to 48.9 and 7.5 MPa, respectively. Based on this technology, Lyu et al. [114] developed 3D printed sandwich-structured porous concrete, which offers higher water drainage or retention permeability, making it ideal for constructing sponge cities [115]. On the other hand, Mai et al. [6] presented Large Particle 3D Concrete Printing, using a large-scale demonstrator to print shotcrete with CAs up to 36 mm diameter, reducing cement

usage by over 50% and increasing compressive strength to 65 MPa. This technology also incorporates the automatic fabrication of prefabricated reinforcement inlays, featuring corrosion-resistant glass fibre roving with an epoxy resin coating [116].

Compared with extrusion-based 3DCP, the most significant advantage of CAB is using more CAs without concerning blocking issues, achieved through the separation feeds of CA and cement. Satisfactory buildability and the ability to print overhangs can be also achieved due to the mechanical stability of CAs [17,117].

The main challenge of the CAB technique is controlling paste penetration into CAs, crucial for strength and shape accuracy. Complete penetration ensures robust layers and prevents anisotropic behaviour. To achieve this, the paste requires sufficient fluidity with a relatively low yield stress and plastic viscosity. Excessively yield stress results in elliptical layer shape, decreasing accuracy, while too low yield stress weakens bonding. Higher plastic viscosity increases coarse air void volume, reducing overall strength. Analytical methods were proposed to predict the penetration depth based on the material properties and driving pressure gradient [112,118]. To balance penetration and skeleton strength, a water-cement ratio of 0.4 and a sand-cement ratio of 1.0 were recommended to maintain moderate yield stress and relatively low plastic viscosity [18].

6. Challenges and future directions

While there have been some advancements in integrating CAC into 3DCP, challenges remain, careful consideration of the mixture design for 3D printable CAC is essential to achieve the desired printability. Most research utilised empirical methods but there are no design codes and standards established yet. To further optimise mixture design, further studied are suggested to conduct as follows:

- The effects of CA content on yield strength need to be clarified, especially for the volume content in a range of 6.1% to 18.3%.
- To determine the optimal cement/paste content and aggregate gradation, novel quantitative mixture design approaches and formulations, such as those discussed in literature [29,64], should be developed.
- The plastic viscosity of CAC needs to be further reduced by implementing novel additives or adjusting aggregate gradation.
- Short open time and a limited understanding of durability are two crucial factors affecting the application of RAC, which is valued for excellent buildability and

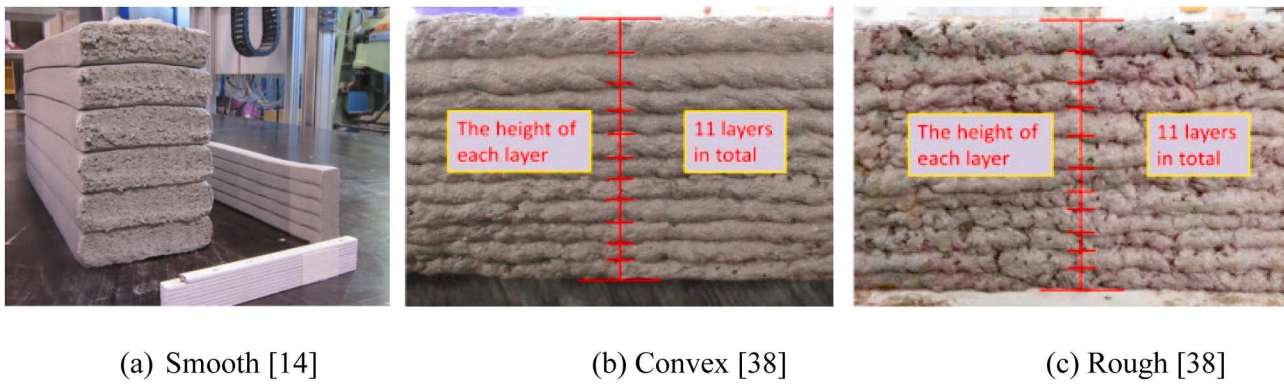


Figure 13. Three levels of surface quality of 3D printed CAC structures.

sustainability. The former issue may be alleviated by using various additives or compensated mixes with SSD aggregates.

While novel pumping and extrusion technologies have been proposed for continuous CAC delivery, they may increase printhead weight and reduce positioning accuracy. Practical construction issues, such as pump wear and material blockages, often disrupt the printing process. Solutions may involve developing optimised drive components, control algorithms, and systems to enhance printing precision and system robustness [14].

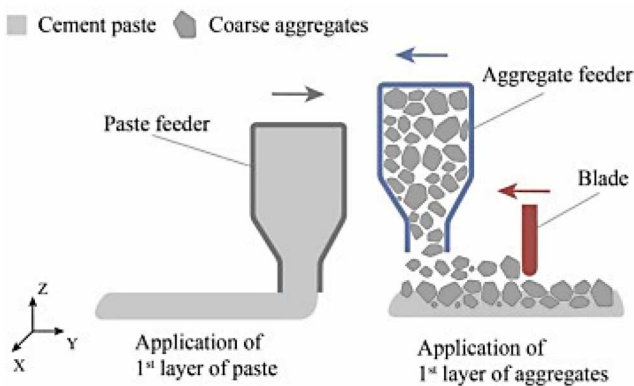
Regarding 3D printed CAC structures, further investigation is needed on stiffness-based failure criteria. Practical applications of large-scale on-site 3D printed CAC structures are still limited, mainly due to challenges in placing reinforcement, which is currently performed manually. The placing method and automatic lay-up of steel reinforcement during 3D printing process, such as steel printing [119] and fibre reinforcement [78], would significantly improve the construction speed

with providing a much more efficient alternative construction approach for industry.

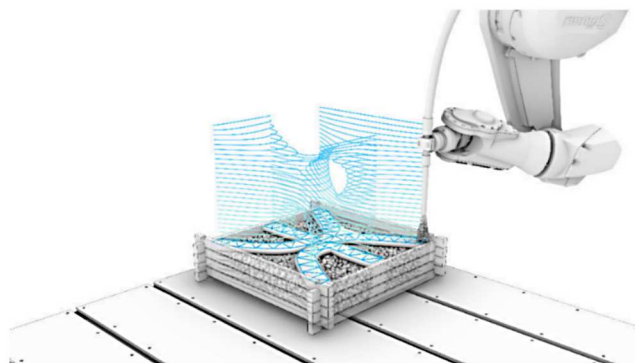
7. Concluding remarks

The paper presents a comprehensive review of two prominent 3DPCAC technologies: extrusion-based and particle-bed concrete printing. Incorporating CAC into extrusion-based 3DCP is examined across three perspectives: 3D printable material, 3D printing process, and 3D printed structures. From this review, the following conclusions can be drawn:

- CAs improve buildability but pose challenges for pumpability and extrudability due to high yield stress, plastic viscosity, and internal friction angle. Careful considerations are required for an optimal mixture design to achieve desired rheological and mechanical behaviours and printable requirements.
- Novel pumping and extrusion technologies, along with two-stage material handling, have been



(a) Aggregate-bed 3D concrete printing [17]



(b) Large particle 3D concrete printing [6]

Figure 14. CAB technologies.

successfully proposed to transport CAC smoothly. Vertical rectangular nozzles with scrapers can provide superior mechanical behaviours and surface quality of printed concrete.

- CAs reduce anisotropy and enhance the mechanical properties of 3D printed concrete, including compressive, flexural, and interlayer bond splitting tensile strengths, as well as elastic modulus.
- 3D printed CAC structures exhibit higher printing heights to prevent early elastic buckling and plastic collapse and different compression failure modes compared to mortar structures. To prevent premature elastic buckling, higher elastic modulus and precise printing control are essential.
- With the incorporation of reinforcement into 3DPCAC, large-scale 3D printed concrete structures that withstand structural loads in design codes can be achieved. It offers improved structural behaviours, cost-effectiveness and sustainability compared to 3D printed mortar structures. Automated steel reinforcement applications and standardised construction methods would boost industrial advancement.
- The CAB process allows for printing concrete with a high content of CA (40%). The main challenge lies in effectively controlling paste penetration into CAs.

Disclosure statement

No potential conflict of interest was reported by the author(s).

Funding

This work was supported by China Scholarship Council: [Grant Number 202008370196].

Data availability statement

Data availability is not applicable to this article as no new data were created or analysed in this study.

ORCID

Dong An  <http://orcid.org/0009-0003-9939-8441>

Y.X. Zhang  <http://orcid.org/0000-0003-1912-8277>

Richard (Chunhui) Yang  <http://orcid.org/0000-0001-5598-958X>

References

[1] Mechtcherine V, Bos FP, Perrot A, et al. Extrusion-based additive manufacturing with cement-based materials – production steps, processes, and their underlying physics: a review. *Cem Concr Res.* 2020;132:106037. doi:10.1016/j.cemconres.2020.106037

[2] Hou S, Duan Z, Xiao J, et al. A review of 3D printed concrete: performance requirements, testing measurements and mix design. *Constr Build Mater.* 2021;273:121745.

[3] Şahin HG, Mardani-Aghabaglou A. Assessment of materials, design parameters and some properties of 3D printing concrete mixtures; a state-of-the-art review. *Constr Build Mater.* 2022;316:125865. doi:10.1016/j.conbuildmat.2021.125865

[4] Tay YWD, Panda B, Paul SC, et al. 3D printing trends in building and construction industry: a review. *Virtual Phys Prototyp.* 2017;12(3):261–276. doi:10.1080/17452759.2017.1326724

[5] Souza MT, Ferreira IM, Guzi de Moraes E, et al. Novaes de oliveira, 3D printed concrete for large-scale buildings: an overview of rheology, printing parameters, chemical admixtures, reinforcements, and economic and environmental prospects. *J Build Eng.* 2020;32:101833. doi:10.1016/j.jobe.2020.101833

[6] Mai I, Brohmann L, Freund N, et al. Large particle 3D concrete printing-A green and viable solution. *Materials.* 2021;14(20):6125.

[7] Xiao J, Ji G, Zhang Y, et al. Large-scale 3D printing concrete technology: current status and future opportunities. *Cem Concr Compos.* 2021;122. doi:10.1016/j.cemconcomp.2021.104115

[8] Tay YWD, Lim JH, Li M, et al. Creating functionally graded concrete materials with varying 3D printing parameters. *Virtual Phys Prototyp.* 2022;17(3):662–681. doi:10.1080/17452759.2022.2048521

[9] Gebhard L, Burger J, Mata-Falcón J, et al. Towards efficient concrete structures with ultra-thin 3D printed formwork: exploring reinforcement strategies and optimisation. *Virtual Phys Prototyp.* 2022;17(3):599–616. doi:10.1080/17452759.2022.2041873

[10] Bai G, Wang L, Ma G, et al. 3D printing eco-friendly concrete containing under-utilised and waste solids as aggregates. *Cem Concr Compos.* 2021;120:104037.

[11] Chen Y, Zhang Y, Pang B, et al. Extrusion-based 3D printing concrete with coarse aggregate: printability and direction-dependent mechanical performance. *Constr Build Mater.* 2021;296:123624.

[12] Rahul AV, Mohan MK, Schutter GD, et al. 3D printable concrete with natural and recycled coarse aggregates: rheological, mechanical and shrinkage behaviour. *Cem Concr Compos.* 2022;125. doi:10.1016/j.cemconcomp.2021.104311

[13] Ashrafi N, Duarte JP, Nazarian S, et al. Evaluating the relationship between deposition and layer quality in large-scale additive manufacturing of concrete. *Virtual Phys Prototyp.* 2019;14(2):135–140. doi:10.1080/17452759.2018.1532800

[14] Mechtcherine V, Nerella VN, Will F, et al. Large-scale digital concrete construction – CONPrint3D concept for on-site, monolithic 3D-printing. *Autom Constr.* 2019;107:102933. doi:10.1016/j.autcon.2019.102933

[15] Mohan MK, Rahul AV, van Dam B, et al. Performance criteria, environmental impact and cost assessment for 3D printable concrete mixtures. *Resour Conserv Recycl.* 2022;181; doi:10.1016/j.resconrec.2022.106255

[16] Tay YWD, Lim SG, Phua SLB, et al. Exploring carbon sequestration potential through 3D concrete printing.

- Virtual Phys Prototyp. 2023;18(1):e2277347. doi:10.1080/17452759.2023.2277347
- [17] Yu S, Du H, Sanjayan J. Aggregate-bed 3D concrete printing with cement paste binder. *Cem Concr Res*. 2020;136:106169.
- [18] Yu S, Sanjayan J, Du H. Effects of cement mortar characteristics on aggregate-bed 3D concrete printing. *Addi Manuf*. 2022;58:103024.
- [19] Liu H, Liu C, Wu Y, et al. 3D printing concrete with recycled coarse aggregates: the influence of pore structure on interlayer adhesion. *Cem Concr Compos*. 2022;134:104742.
- [20] Liu H, Liu C, Wu Y, et al. Hardened properties of 3D printed concrete with recycled coarse aggregate. *Cem Concr Res*. 2022;159:106868.
- [21] Chen W, Jin R, Xu Y, et al. Adopting recycled aggregates as sustainable construction materials: a review of the scientific literature. *Constr Build Mater*. 2019;218:483–496. doi:10.1016/j.conbuildmat.2019.05.130
- [22] Ahmed GH. A review of “3D concrete printing”: materials and process characterization, economic considerations and environmental sustainability. *J Build Eng*. 2023;66:105863. doi:10.1016/j.jobe.2023.105863
- [23] Zhao Z, Ji C, Xiao J, et al. A critical review on reducing the environmental impact of 3D printing concrete: material preparation, construction process and structure level. *Constr Build Mater*. 2023;409:133887.
- [24] Ji G, Xiao J, Zhi P, et al. Effects of extrusion parameters on properties of 3D printing concrete with coarse aggregates. *Constr Build Mater*. 2022;325:126740.
- [25] Liu H, Liu C, Bai G, et al. Influence of pore defects on the hardened properties of 3D printed concrete with coarse aggregate. *Addi Manuf*. 2022;55:102843.
- [26] Taubert M, Mechtcherine V. Mix design for a 3D-printable concrete with coarse aggregates and consideration of standardisation. *Third RILEM International Conference on Concrete and Digital Fabrication*; 2022. p. 59–64.
- [27] Wang X, Jia L, Jia Z, et al. Optimization of 3D printing concrete with coarse aggregate via proper mix design and printing process. *J Build Eng*. 2022;56:104745.
- [28] Xiao J, Lv Z, Duan Z, et al. Study on preparation and mechanical properties of 3D printed concrete with different aggregate combinations. *J Build Eng*. 2022;51:104282. doi:10.1016/j.jobe.2022.104282
- [29] Zhang C, Jia Z, Wang X, et al. A two-phase design strategy based on the composite of mortar and coarse aggregate for 3D printable concrete with coarse aggregate. *J Build Eng*. 2022;54:104672.
- [30] Chen Y, Zhang W, Zhang Y, et al. 3D printed concrete with coarse aggregates: built-in-stirrup permanent concrete formwork for reinforced columns. *J Build Eng*. 2023;70:106362.
- [31] Seo E-A, Kim W-W, Kim S-W, et al. Mechanical properties of 3D printed concrete with coarse aggregates and polypropylene fiber in the air and underwater environment. *Constr Build Mater*. 2023;378:131184.
- [32] Vespalec A, Podrouzek J, Boštík J, et al. Experimental study on time dependent behaviour of coarse aggregate concrete mixture for 3D construction printing. *Constr Build Mater*. 2023;376:130999. doi:10.1016/j.conbuildmat.2023.130999
- [33] Vespalec A, Podrouzek J, Koutny D. Doe approach to setting input parameters for digital 3D printing of concrete for coarse aggregates up to 8 mm. *Materials*. 2023;16(9). doi:10.3390/ma16093418
- [34] Sasikumar A, Balasubramanian D, Senthil Kumaran MS, et al. Effect of coarse aggregate content on the rheological and buildability properties of 3D printable concrete. *Constr Build Mater*. 2023;392:131859. doi:10.1016/j.conbuildmat.2023.131859
- [35] Jiao D, Shi C, Yuan Q, et al. Effect of constituents on rheological properties of fresh concrete-A review. *Cem Concr Compos*. 2017;83:146–159. doi:10.1016/j.cemconcomp.2017.07.016
- [36] Jayathilakage R, Rajeev P, Sanjayan JG. Yield stress criteria to assess the buildability of 3D concrete printing. *Constr Build Mater*. 2020;240:117989. doi:10.1016/j.conbuildmat.2019.117989
- [37] Nerella VN, Beigh MAB, Fataei S, et al. Strain-based approach for measuring structural build-up of cement pastes in the context of digital construction. *Cem Concr Res*. 2019;115:530–544. doi:10.1016/j.cemconres.2018.08.003
- [38] Wu Y, Liu C, Liu H, et al. Study on the rheology and buildability of 3D printed concrete with recycled coarse aggregates. *J Build Eng*. 2021;42:103030.
- [39] Ivanova I, Mechtcherine V. Possibilities and challenges of constant shear rate test for evaluation of structural build-up rate of cementitious materials. *Cem Concr Res*. 2020;130:105974. doi:10.1016/j.cemconres.2020.105974
- [40] Perrot A, Rangeard D, Pierre A. Structural built-up of cement-based materials used for 3D-printing extrusion techniques. *Mater Struct*. 2016;49(4):1213–1220. doi:10.1617/s11527-015-0571-0
- [41] Wangler T, Lloret E, Reiter L, et al. Digital concrete: opportunities and challenges. *RILEM Tech Lett*. 2016;1:67–75. doi:10.21809/rilemtechlett.2016.16
- [42] Mahaut F, Mokéddem S, Chateau X, et al. Effect of coarse particle volume fraction on the yield stress and thixotropy of cementitious materials. *Cem Concr Res*. 2008;38(11):1276–1285. doi:10.1016/j.cemconres.2008.06.001
- [43] Subramaniam KV, Wang X. An investigation of microstructure evolution in cement paste through setting using ultrasonic and rheological measurements. *Cem Concr Res*. 2010;40(1):33–44. doi:10.1016/j.cemconres.2009.09.018
- [44] Perrot A, Pierre A, Vitaloni S, et al. Prediction of lateral form pressure exerted by concrete at low casting rates. *Mater Struct*. 2015;48(7):2315–2322. doi:10.1617/s11527-014-0313-8
- [45] Rahul AV, Santhanam M. Evaluating the printability of concretes containing lightweight coarse aggregates. *Cem Concr Compos*. 2020;109:103570. doi:10.1016/j.cemconcomp.2020.103570
- [46] Mahaut F, Chateau X, Coussot P, et al. Yield stress and elastic modulus of suspensions of noncolloidal particles in yield stress fluids. *J Rheol*. 2008;52(1):287–313. doi:10.1122/1.2798234
- [47] Noor TUMA. Rheology of high flowing mortar and concrete. *Mater Struct*. 2004;37:513–521. doi:10.1007/BF02481575

- [48] Cui H, Li Y, Cao X, et al. Experimental study of 3D concrete printing configurations based on the buildability evaluation. *Appl Sci*. 2022;12(6):2939.
- [49] Reinhardt HW, Wüstholtz T. About the influence of the content and composition of the aggregates on the rheological behaviour of self-compacting concrete. *Mater Struct*. 2006;39(7):683–693. doi:10.1617/s11527-006-9102-3
- [50] Yammine J, Chaouche M, Guerin M, et al. From ordinary rheology concrete to self compacting concrete: a transition between frictional and hydrodynamic interactions. *Cem Concr Res*. 2008;38(7):890–896. doi:10.1016/j.cemconres.2008.03.011
- [51] Xiao J, Hou S, Duan Z, et al. Rheology of 3D printable concrete prepared by secondary mixing of ready-mix concrete. *Cem Concr Compos*. 2023;138:104958. doi:10.1016/j.cemconcomp.2023.104958
- [52] Silva RV, de Brito J, Dhir RK. Fresh-state performance of recycled aggregate concrete: a review. *Constr Build Mater*. 2018;178:19–31. doi:10.1016/j.conbuildmat.2018.05.149
- [53] Seara-Paz S, González-Fontebao B, Martínez-Abella F, et al. Deformation recovery of reinforced concrete beams made with recycled coarse aggregates. *Eng Struct*. 2022;251:113482. doi:10.1016/j.engstruct.2021.113482
- [54] Tong J, Ding Y, Lv X, et al. Effect of carbonated recycled coarse aggregates on the mechanical properties of 3D printed recycled concrete. *J Build Eng*. 2023;80:107959. doi:10.1016/j.jobte.2023.107959
- [55] Roussel N. Rheological requirements for printable concretes. *Cem Concr Res*. 2018;112:76–85. doi:10.1016/j.cemconres.2018.04.005
- [56] Mechtcherine V, Nerella VN, Kasten K. Testing pumpability of concrete using sliding pipe rheometer. *Constr Build Mater*. 2014;53:312–323. doi:10.1016/j.conbuildmat.2013.11.037
- [57] He L, Tan JZM, Chow WT, et al. Design of novel nozzles for higher interlayer strength of 3D printed cement paste. *Addit Manuf*. 2021;48:102452.
- [58] Bong SH, Xia M, Nematollahi B, et al. Ambient temperature cured 'just-add-water' geopolymer for 3D concrete printing applications. *Cem Concr Compos*. 2021;121:104060.
- [59] Le TT, Austin SA, Lim S, et al. Mix design and fresh properties for high-performance printing concrete. *Mater Struct*. 2012;45(8):1221–1232. doi:10.1617/s11527-012-9828-z
- [60] Nerella VN, Näther M, Iqbal A, et al. Inline quantification of extrudability of cementitious materials for digital construction. *Cem Concr Compos*. 2019;95:260–270. doi:10.1016/j.cemconcomp.2018.09.015
- [61] El Cheikh K, Rémond S, Khalil N, et al. Numerical and experimental studies of aggregate blocking in mortar extrusion. *Constr Build Mater*. 2017;145:452–463. doi:10.1016/j.conbuildmat.2017.04.032
- [62] Ahmed ZY, Bos FP, Van Brunschot M, et al. On-demand additive manufacturing of functionally graded concrete. *Virtual Phys Prototyp*. 2020;15(2):194–210. doi:10.1080/17452759.2019.1709009
- [63] Rushing TS, Stynoski PB, Barna LA, et al. Investigation of concrete mixtures for additive construction. In *3D concrete printing technology*. Elsevier; 2019, p. 137–160.
- [64] Taubert M, Mechtcherine V. Mix design for a 3D-printable concrete with coarse aggregates and consideration of standardisation. *Rilem International Conference on Concrete and Digital Fabrication*. Springer; 2022, p. 59–64.
- [65] Ji G, Ding T, Xiao J, et al. A 3D printed ready-mixed concrete power distribution substation. *Mater Constr Technol Mater*. 2019;12(9):1540.
- [66] Vespalec A, Novak J, Kohoutkova A, et al. Interface behavior and interface tensile strength of a hardened concrete mixture with a coarse aggregate for additive manufacturing. *Materials*. 2020;13(22). doi:10.3390/ma13225147
- [67] Liu Y, Wang L, Yuan Q, et al. Effect of coarse aggregate on printability and mechanical properties of 3D printed concrete. *Constr Build Mater*. 2023;405:133338.
- [68] Hüsken G, Brouwers HJH. On the early-age behavior of zero-slump concrete. *Cem Concr Res*. 2012;42(3):501–510. doi:10.1016/j.cemconres.2011.11.007
- [69] Güllü H, Agha AA. The rheological, fresh and strength effects of cold-bonded geopolymer made with meta-kaolin and slag for grouting. *Constr Build Mater*. 2021;274. doi:10.1016/j.conbuildmat.2020.122091
- [70] Duan Z, Hou S, Xiao J, et al. Study on the essential properties of recycled powders from construction and demolition waste. *J Clean Prod*. 2020;253:119865. doi:10.1016/j.jclepro.2019.119865
- [71] Bos F, Bosco E, Salet T. Ductility of 3D printed concrete reinforced with short straight steel fibers. *Virtual Phys Prototyp*. 2019;14(2):160–174. doi:10.1080/17452759.2018.1548069
- [72] Rahman M, Baluch M, Malik M. Thixotropic behavior of self compacting concrete with different mineral admixtures. *Constr Build Mater*. 2014;50:710–717. doi:10.1016/j.conbuildmat.2013.10.025
- [73] Benaicha M, Roguiez X, Jalbaud O, et al. Influence of silica fume and viscosity modifying agent on the mechanical and rheological behavior of self compacting concrete. *Constr Build Mater*. 2015;84:103–110. doi:10.1016/j.conbuildmat.2015.03.061
- [74] Burroughs JF, Weiss J, Haddock JE. Influence of high volumes of silica fume on the rheological behavior of oil well cement pastes. *Constr Build Mater*. 2019;203:401–407. doi:10.1016/j.conbuildmat.2019.01.027
- [75] Zhang X, Han J. The effect of ultra-fine admixture on the rheological property of cement paste. *Cem Concr Res*. 2000;30(5):827–830. doi:10.1016/S0008-8846(00)00236-2
- [76] Ahari RS, Erdem TK, Ramyar K. Effect of various supplementary cementitious materials on rheological properties of self-consolidating concrete. *Constr Build Mater*. 2015;75:89–98. doi:10.1016/j.conbuildmat.2014.11.014
- [77] Chen Y, Zhang Y, Pang B, et al. Steel fiber orientational distribution and effects on 3D printed concrete with coarse aggregate. *Mater Struct*. 2022;55(3):100. doi:10.1617/s11527-022-01943-7
- [78] Zhou Y, Jiang D, Sharma R, et al. Enhancement of 3D printed cementitious composite by short fibers: a review. *Constr Build Mater*. 2023;362:129763.
- [79] Zhang D, Feng P, Zhou P, et al. 3D printed concrete walls reinforced with flexible FRP textile: automatic

- construction, digital rebuilding, and seismic performance. *Eng Struct.* 2023;291:116488.
- [80] Shakor P, Nejadi S, Paul G, et al. Review of emerging additive manufacturing technologies in 3D printing of cementitious materials in the construction industry. *Front Built Environ.* 2019;4. doi:10.3389/fbuil.2018.00085
- [81] Muthukrishnan S, Ramakrishnan S, Sanjayan J. Technologies for improving buildability in 3D concrete printing. *Cem Concr Compos.* 2021;122:104144. doi:10.1016/j.cemconcomp.2021.104144
- [82] Zhang C, Wang H. Swing vibration control of suspended structures using the active rotary inertia driver system: theoretical modeling and experimental verification. *Struc Contr Health Monit.* 2020;27(6):e2543.
- [83] Perrot A, Rangeard D, Courteille E. 3D printing of earth-based materials: processing aspects. *Constr Build Mater.* 2018;172:670–676. doi:10.1016/j.conbuildmat.2018.04.017
- [84] Bos F, Wolfs R, Ahmed Z, et al. Additive manufacturing of concrete in construction: potentials and challenges of 3D concrete printing. *Virtual Phys Prototyp.* 2016;11(3):209–225. doi:10.1080/17452759.2016.1209867
- [85] Salet TAM, Ahmed ZY, Bos FP, et al. Design of a 3D printed concrete bridge by testing. *Virtual Phys Prototyp.* 2018;13(3):222–236. doi:10.1080/17452759.2018.1476064
- [86] Zareiyan B, Khoshnevis B. Effects of interlocking on inter-layer adhesion and strength of structures in 3D printing of concrete. *Autom Constr.* 2017;83:212–221. doi:10.1016/j.autcon.2017.08.019
- [87] Pattaje Sooryanarayana K, Stynoski P, Lange D. Effect of vibration on the rheology of concrete for 3D printing, Second RILEM International Conference on Concrete and Digital Fabrication; 2020, p. 353–359.
- [88] Controlling Three-Dimensional-Printable Concrete with Vibration. *ACI Mater J.* 2021;118(6):353–358.
- [89] Khoshnevis B. Automated construction by contour crafting—related robotics and information technologies. *Autom Constr.* 2004;13(1):5–19. doi:10.1016/j.autcon.2003.08.012
- [90] Akcay B, Agar-Ozbek AS, Bayramov F, et al. Interpretation of aggregate volume fraction effects on fracture behavior of concrete. *Constr Build Mater.* 2012;28(1):437–443. doi:10.1016/j.conbuildmat.2011.08.080
- [91] Warsi SBF, Srinivas D, Panda B, et al. Investigating the impact of coarse aggregate dosage on the mechanical performance of 3D printable concrete. *Innovative Infrastructure Solutions.* 2024;9(1):5. doi:10.1007/s41062-023-01317-0
- [92] Ali A, Riaz RD, Malik UJ, et al. Machine learning-based predictive model for tensile and flexural strength of 3D-printed concrete. *Materials.* 2023;16(11):4149.
- [93] Tay YWD, Ting GHA, Qian Y, et al. Time gap effect on bond strength of 3D-printed concrete. *Virtual Phys Prototyp.* 2019;14(1):104–113. doi:10.1080/17452759.2018.1500420
- [94] Ye J, Cui C, Yu J, et al. Effect of polyethylene fiber content on workability and mechanical-anisotropic properties of 3D printed ultra-high ductile concrete. *Constr Build Mater.* 2021;281:122586.
- [95] Kalra M, Mehmood G. A review paper on the effect of different types of coarse aggregate on concrete. *IOP Conf Ser: Mater Sci Eng.* 2018;431:082001. doi:10.1088/1757-899X/431/8/082001
- [96] Suiker A. Mechanical performance of wall structures in 3D printing processes: theory, design tools and experiments. *Int J Mech Sci.* 2018;137:145–170. doi:10.1016/j.ijmecsci.2018.01.010
- [97] Panda B, Lim JH, Tan MJ. Mechanical properties and deformation behaviour of early age concrete in the context of digital construction. *Compos Part B: Eng.* 2019;165:563–571. doi:10.1016/j.compositesb.2019.02.040
- [98] Dell'Endice A, Bouten S, Van Mele T, et al. Structural design and engineering of StriatuS, an unreinforced 3D-concrete-printed masonry arch bridge. *Eng Struct.* 2023;292:116534. doi:10.1016/j.engstruct.2023.116534
- [99] Mogra M, Asaf O, Sprecher A, et al. Design optimization of 3D printed concrete elements considering buildability. *Eng Struct.* 2023;294:116735. doi:10.1016/j.engstruct.2023.116735
- [100] Anton A, Reiter L, Wangler T, et al. A 3D concrete printing prefabrication platform for bespoke columns. *Autom Constr.* 2021;122:103467. doi:10.1016/j.autcon.2020.103467
- [101] Chen Y, Zhang Y, Liu Z, et al. 3D-printed concrete permanent formwork: effect of postcast concrete proportion on interface bonding. *Mater Lett.* 2023;344:134472.
- [102] Kreiger EL, Kreiger MA, Case MP. Development of the construction processes for reinforced additively constructed concrete. *Addit Manuf.* 2019;28:39–49. doi:10.1016/j.addma.2019.02.015
- [103] Diggs-McGee BN, Kreiger EL, Kreiger MA, et al. Print time vs. elapsed time: a temporal analysis of a continuous printing operation for additive constructed concrete. *Addit Manuf.* 2019;28:205–214. doi:10.1016/j.addma.2019.04.008
- [104] Mueller RP, Fikes JC, Case MP, et al. Additive construction with mobile emplacement (ACME), International Astronautical Federation (IAF), 2017.
- [105] Scott C. Chinese construction company 3D prints an entire two-story house on-site in 45 days, June, 16, 2016. <https://3dprint.com/138664/huashang-tengda-3d-print-house/>.
- [106] Liu H, Liu C, Zhang Y, et al. Bonding properties between 3D printed coarse aggregate concrete and rebar based on interface structural characteristics. *Addit Manuf.* 2023;78:103893. doi:10.1016/j.addma.2023.103893
- [107] Severson B. Shanghai-based WinSun 3D prints 6-story apartment building and an incredible home, January 18, 2015. <https://3dprint.com/38144/3d-printed-apartment-building/>.
- [108] Han Y, Yang Z, Ding T, et al. Environmental and economic assessment on 3D printed buildings with recycled concrete. *J Clean Prod.* 2021;278:123884. doi:10.1016/j.jclepro.2020.123884
- [109] Kazemian A, Yuan X, Cochran E, et al. Cementitious materials for construction-scale 3D printing: laboratory testing of fresh printing mixture. *Constr Build Mater.* 2017;145:639–647. doi:10.1016/j.conbuildmat.2017.04.015
- [110] Holt E, Leivo M. Cracking risks associated with early age shrinkage. *Cem Concr Compos.* 2004;26(5):521–530. doi:10.1016/S0958-9465(03)00068-4

- [111] Eguchi K, Teranishi K. Prediction equation of drying shrinkage of concrete based on composite model. *Cem Concr Res.* 2005;35(3):483–493. doi:[10.1016/j.cemconres.2004.08.002](https://doi.org/10.1016/j.cemconres.2004.08.002)
- [112] Lowke D, Mai I, Keita E, et al. Material-process interactions in particle bed 3D printing and the underlying physics. *Cem Concr Res.* 2022;156. doi:[10.1016/j.cemconres.2022.106748](https://doi.org/10.1016/j.cemconres.2022.106748)
- [113] Lowke D, Dini E, Perrot A, et al. Particle-bed 3D printing in concrete construction – possibilities and challenges. *Cem Concr Res.* 2018;112:50–65. doi:[10.1016/j.cemconres.2018.05.018](https://doi.org/10.1016/j.cemconres.2018.05.018)
- [114] Lyu Q, Dai P, Chen A. Sandwich-structured porous concrete manufactured by mortar-extrusion and aggregate-bed 3D printing. *Constr Build Mater.* 2023; 392:131909.
- [115] Yang M, Chen D, Shi L, et al. How do construct a sponge city that can improve residents' satisfaction? evidence from a suburb of huizhou city, China. *Ecol Indic.* 2022;142:109238.
- [116] Hack N, Bahar M, Hühne C, et al. Development of a robot-based multi-directional dynamic fiber winding process for additive manufacturing using shotcrete 3D printing. *Fibers.* 2021;9(6). doi:[10.3390/fib9060039](https://doi.org/10.3390/fib9060039)
- [117] Pierre A, Weger D, Perrot A, et al. Penetration of cement pastes into sand packings during 3D printing: analytical and experimental study. *Mater Struct.* 2018;51(1). doi:[10.1617/s11527-018-1148-5](https://doi.org/10.1617/s11527-018-1148-5)
- [118] Chevalier T, Chevalier C, Clain X, et al. Darcy's law for yield stress fluid flowing through a porous medium. *J Nonnewton Fluid Mech.* 2013;195:57–66. doi:[10.1016/j.jnnfm.2012.12.005](https://doi.org/10.1016/j.jnnfm.2012.12.005)
- [119] Wu Z, Memari AM, Duarte JP. State of the art review of reinforcement strategies and technologies for 3D printing of concrete. *Energies.* 2022;15(1):360. doi:[10.3390/en15010360](https://doi.org/10.3390/en15010360)